Spin Density Maps in Nitroxide–Copper(II) Complexes. A Polarized Neutron Diffraction Determination[1]

Eric Ressouche,[2a] Jean-Xavier Boucherle,[2a] Béatrice Gillon,[2b] Paul Rey,*[,2a] and Jacques Schweizer*[,2a]

Contribution from the Laboratoire de Chimie de Coordination (URA CNRS 1194), Service d'Etude des Systèmes et Architectures Moléculaires (UA CNRS 1194), and the Service de Physique Statistique, de Magnétisme et de Supraconductivité, Département de Recherche Fondamentale sur la Matière Condensée, Centre d'Etudes Nucléaires de Grenoble, 38041 Grenoble Cedex, France, and Laboratoire Léon Brillouin (CEA-CNRS), Centre d'Etudes Nucléaires de Saclay, 91191 Gif-Sur-Yvette, France

Received September 1, 1992

Abstract: Low-temperature crystal structures and spin density distributions in two copper(II)–nitronyl nitroxide complexes have been determined by neutron diffraction experiments. The first complex, catena(μ-1,3-(2,4,4,5,5-pentamethyl-4,5-dihydro-1*H*-imidazolyl-1-oxyl 3-oxide)bis(hexafluoroacetylacetonato)copper(II)) ($(Cu(hfac)_2NITMe)_n$, **1**), is a linear chain species of alternating radicals and metal ions where the metal–radical interaction is ferromagnetic. In contrast, bis(2-phenyl-4,4,5,5-tetramethyl-4,5-dihydro-1*H*-imidazolyl-1-oxyl 3-oxide)copper(II) chloride ($CuCl_2(NITPh)_2$, **2**) is a discrete centrosymmetric bis-nitroxide adduct exhibiting a strong metal–nitroxide antiferromagnetic coupling. For **2**, the low- and high-temperature molecular structures are identical while in **1**, at low temperature, a shortening of the interchain distance and a folding of the metal–acetylacetonato rings are observed. Spin density distribution maps were determined at 2.5 K for **1** and 13 K for **2**; they were found to be in qualitative and quantitative agreement with the ground state of both compounds. In **1**, the spin density is positive throughout the molecular backbone in agreement with the observed metal–radical ferromagnetic interaction. In **2**, the antiferromagnetic behavior is reflected in spin densities of opposite signs on the organic radicals and on the metal ion; the ratio of these densities (−1/2) allows an unambigous description of the ground doublet state of this three-spin system. Examination of the unpaired spin distribution on the various fragments of both compounds clearly indicates that binding induces a shift of the spin density from the oxygen to the nitrogen in the nitroxide group. This effect is more pronounced in **2** where the radical is stronger bound than in **1** where the metal–oxygen bond is weak. The vanishingly small density on the bonded nitroxyl oxygen in **2** is probably a consequence of such a redistribution, although compensation between opposite contributions cannot be excluded. In **1**, the copper centers have predominant $d_{x^2-y^2}$ character while in the nitroxide a strong departure from the ideal π^* description is observed. The magnetic orbital is tilted from the $2p_z$ direction resulting in a favorable arrangement for weak overlap and ferromagnetic coupling.

Metal–nitroxide complexes currently attract much interest because direct binding of the organic free radical to a metal ion is an optimum scheme for obtaining exchange-coupled species.[3-6] Some of these derivatives are extended linear molecules exhibiting remnant magnetization at low temperature.[7,8] In the recent past, however, the coordination chemistry of nitroxides has focussed on the preparation of discrete complexes; a thorough study of these simple systems was needed to understand the metal–radical exchange mechanisms and to draw out magneto–structural correlations[9,10] allowing the design of compounds exhibiting bulk magnetic properties.

Most preliminary studies have been devoted to copper(II) derivatives. In copper(II) complexes, the symmetry of the magnetic orbital strongly depends on the geometry of the coordination sphere. Because of the great diversity of the copper coordination polyhedra and depending on the binding geometry of the nitroxide ligand, many different structural arrangements and coupling schemes are possible. Indeed, dramatically different magnetic behaviors have been observed: Schematically, complexes with *short-bonded equatorial* nitroxide ligands exhibit strong antiferromagnetic couplings,[4,11,12] while those containing a *long-bonded axial* nitroxide exhibit a ferromagnetic behavior.[9,13-16] It has been shown that overlap of the metal and radical magnetic orbitals is efficient in the first case, while these orbitals are quasiorthogonal in the second case.[9] This rationalization of the magnetic properties of copper(II)–nitroxide complexes is supported by the currently accepted theoretical description of the interactions between paramagnetic centers using natural magnetic orbitals.[17]

These qualitative considerations rely on both structural and electronic features of the non-interacting fragments. However, it is known that even in unconjugated nitroxides like 2,2,6,6-tetramethylpiperidine-1-oxyl (Tempo) where the unpaired spin population is strongly localized in a π^* orbital on the NO group, the involvement of the oxygen atom in weak interactions such as

(1) Part of the Doctoral thesis of E. Ressouche.
(2) (a) CEN Grenoble. (b) CEN Saclay.
(3) Lim, Y. Y.; Drago, R. S. *Inorg. Chem.* **1972**, *11*, 1334–1338.
(4) Dickman, M. H.; Doedens, R. J. *Inorg. Chem.* **1981**, *20*, 2677–2681.
(5) Caneschi, A.; Gatteschi, D.; Sessoli, R.; Rey, P. *Acc. Chem. Res.* **1989**, *22*, 392–398.
(6) Caneschi, A.; Gatteschi, D.; Rey, P. *Progr. Inorg. Chem.* **1991**, *39*, 331–429.
(7) Caneschi, A.; Gatteschi, D.; Renard, J.-P.; Rey, P.; Sessoli, R. *Inorg. Chem.* **1989**, *28*, 1976–1980.
(8) Caneschi, A.; Gatteschi, D.; Renard, J.-P.; Rey, P.; Sessoli, R. *Inorg. Chem.* **1989**, *28*, 2940–2944.
(9) Caneschi, A.; Gatteschi, D.; Grand, A.; Laugier, J.; Pardi, L. Rey, P. *Inorg. Chem.* **1988**, *27*, 1031–1035.
(10) Caneschi, A.; Gatteschi, D.; Laugier, J.; Pardi, L.; Rey, P.; Zanchini, C. *Inorg. Chem.* **1988**, *27*, 2027–2032.
(11) Caneschi, A.; Grand, A.; Laugier, J.; Rey, P.; Subra, R. *J. Am. Chem. Soc.* **1988**, *110*, 2307–2309.
(12) Laugier, J.; Rey, P.; Benelli, C.; Gatteschi, D.; Zanchini, C. *J. Am. Chem. Soc.* **1986**, *108*, 6931–6937.
(13) Grand, A.; Rey, P.; Subra, R. *Inorg. Chem.* **1983**, *22*, 391–394.
(14) Bencini, A.; Benelli, C.; Gatteschi, D.; Zanchini, C. *J. Am. Chem. Soc.* **1984**, *106*, 5813–5818.
(15) Ovcharenko, V. I.; Ikorskii, V. N.; Podberezskaya, N. V.; Pervukhina, N. V.; Larionov, S. V. *Russ. J. Inorg. Chem.* **1987**, *32*, 844–846.
(16) Caneschi, A.; Gatteschi, D.; Laugier, J.; Rey, P. *J. Am. Chem. Soc.* **1987**, *109*, 2191–2192.
(17) Kahn, O. *Angew. Chem., Int. Ed. Engl.* **1985**, *24*, 834–850.

0002-7863/93/1515-3610$04.00/0

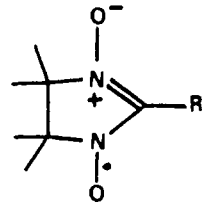

R = Ph, NITPh

R = Me, NITMe

Figure 1. Chemical structure of the nitroxide ligands.

hydrogen bonding induces a modification of the spin distribution.[18] Stronger interactions which occur upon coordination of diamagnetic metal ions have been shown to result in electronic redistribution involving the metal fragment.[19,20] When the ligand is a nitronyl nitroxide (Figure 1), in which the unpaired electron is delocalized on an organic fragment, this reorganization is more pronounced as evidenced by the lengthening of the coordinated NO bond in strongly interacting complexes.[4-6] This set of observations supports the expectation that a strong modification of the starting electronic description has occurred upon complexation.

In order to get a deeper insight into the electronic structures and mechanisms of spin interactions in nitroxide bound species, we have determined the spin density distribution in two copper(II) complexes of nitronyl nitroxides [catena(μ-1,3-(2,4,4,5,5-pentamethyl-4,5-dihydro-1*H*-imidazolyl-1-oxyl 3-oxide)bis(hexafluoroacetylacetonato)copper(II)) ((Cu(hfac)$_2$NITMe)$_n$, **1**) and bis(2-phenyl-4,4,5,5-tetramethyl-4,5-dihydro-1*H*-imidazolyl-1-oxyl 3-oxide) copper(II) chloride ($CuCl_2(NITPh)_2$, **2**)] by using polarized neutron diffraction techniques.[21] These two compounds represent the two classes of complexes. In the hexafluoroacetylacetonate adduct **1**, the bridging nitroxide is axially bound to two metal ions and the coupling is weakly ferromagnetic,[16] while in **2**, the nitroxide ligand is equatorially bound. In the square-planar centrosymmetric complex **2**, the two nitroxide ligands and the copper(II) ion are so strongly antiferromagnetically coupled that even at room temperature the three-spin system behaves as a $S = {}^1/_2$ spin; additional intermolecular interactions between uncoordinated NO groups are responsible for the maximum at 13 K observed in the temperature dependent magnetic susceptibility.[12]

The determination of the spin population in **1** and **2** assesses the respective ground state and gives a clear description of the electronic structure as well as of the coupling mechanisms responsible for the observed magnetic properties.

Experimental Section

Syntheses. Both compounds were obtained as previously described.[12,16] Large crystals suited for a polarized neutron diffraction experiment were obtained as follows: Crystals of compound **1** were grown by slow evaporation at room temperature of pentane solutions of 1/1 mixtures of Cu(hfac)$_2$ and NITMe, while large parallelepipedic crystals of **2** were obtained by keeping a concentrated ethanol solution (0.2 mol/L) at 4 °C for 8 days. For both compounds, the crystal cell and the magnetic properties were checked and found to be identical to those previously reported. In addition, it was observed that slow cooling was necessary to produce crystals of compound **1** at the neutron experiment temperature (13 K) without damage.

Table I. Low- and High-Temperature Cell Parameters for **1** and **2**

	1		**2**	
	T = 10 K	RT	T = 13 K	RT
a (Å)	8.728(21)	8.955(6)	11.887(6)	11.988(4)
b (Å)	15.988(27)	15.915(7)	10.707(6)	10.878(3)
c (Å)	9.052(11)	10.294(4)	14.215(12)	14.286(6)
α (deg)	81.07(9)	79.20(3)		
β (deg)	72.65(11)	68.24(2)	128.14(12)	127.57(8)
γ (deg)	79.25(13)	73.44(3)		

Neutron Diffraction Data Collection and Low-Temperature Structure Determination. Compound 1. This complex crystallizes in space group $P\bar{1}$. One edge of the crystal corresponded to the $\vec{a}$ direction and was vertically set on the D15 lifting-counter single crystal diffractometer located at a thermal source of the Institute Laue-Langevin (ILL) high-flux reactor in Grenoble. The cell parameters were obtained by least-squares fitting of the setting angles of 28 reflections ($8.5 < 2\theta < 44.5$). One of them, c, showed a surprising shortening of 12% upon cooling while the others exhibited only minor variations as shown in Table I. This change in the c parameter is reversible, but as a consequence of such a modification, even after slow cooling, the crystal exhibited a large increase of mosaicity resulting in a strong reduction of the reflection intensities. However, the use of a sophisticated multidetector[22] partially solved this problem in giving correct integrated reflections in the 2θ plane provided that scans as large as 11° were performed. The integrated intensities were obtained using the COLL5 program of data collection[23] and were corrected for absorption due to the incoherent diffusion of the neutron beam by using Cambridge Library programs.[24]

Due to cell deformation, the room temperature atomic positions were not helpful for refining the structure. Therefore, the two copper–hexafluoroacetylacetonato and nitroxide fragments were initially defined as rigid blocks and their positions and orientations refined using the program ORION.[25] In a second step, the methyl and trifluoromethyl groups were allowed to move. Then, standard refinements[26] including the atomic positions obtained in the two preceding steps and isotropic thermal parameters fixed at values observed for related compounds in the same temperature range[18] converged to an acceptable agreement factor.

Compound 2. This compound was reported[12] to crystallize in space group $P2_1/n$. With use of the $P2_1/c$ description of this space group, Laue photographs showed that the crystals exhibited well-defined edges corresponding to the $\vec{a} + \vec{c}$ and $\vec{c} - \vec{b}$ directions. Since the corresponding angle is 62°, most of the reciprocal space would be available if two crystals were oriented in such a way as to be mounted with one of these directions vertical on the neutron diffractometer. The low-temperature cell constants were determined as for compound **1**. As shown in Table II, two sets of reflections corresponding to the two crystals were collected and corrected as described for compound **1**. Refinement of the structure was straightforward, starting with the atomic positions determined at room temperature by X-ray diffraction and using literature reported Fermi lengths.

For both compounds, low and room temperature cell parameters are found in Table I, experimental data collection parameters in Table II, and selected bond lengths and angles in Table III. Atomic coordinates (Tables S1 and S2), complete listing of bond lengths and angles (Tables S3–S6), anisotropic thermal parameters for **2** (Table S7), and structure factors (Tables S8 and S9) are deposited as supplementary material.

Polarized Neutron Diffraction Experiment. Both polarized neutron data collections were obtained on the D3 diffractometer located at a hot source of ILL. A vertical magnetic field of 4.6 T was applied to the samples, and the Bragg reflections were collected with a detector which can be lifted above the horizontal plane. Data were reduced with the help of Cambridge Library programs,[24] and the magnetic structure factors for these centrosymmetric compounds were obtained using the NPOL

(18) Bordeaux, D.; Boucherle, J.-X.; Delley, B.; Gillon, B.; Ressouche, E.; Schweizer, J. *Magnetic Molecular Materials*; Gatteschi, D., Kahn, O., Miller, J. S., Palacio, F., Eds.; Nato ASI Series 198; D. Reidel Publishing Co.: Dordrecht, Netherland, 1990.
(19) Eames, T. B.; Hoffman, B. M. *J. Am. Chem. Soc.* **1971**, *93*, 3141–3146.
(20) Helbert, J. N.; Kopf, P. W.; Piondexter, E. H.; Wagner, B. E. *J. Chem. Soc., Dalton Trans.* **1975**, 998–1006.
(21) Lovesey, S. W. *Theory of Neutron Scattering from Condensed Matter*; Clarendon Press: Oxford, 1984.
(22) Wilkinson, C.; Khamis, H. W.; Stanfield, R. F. D.; Mc Intyre, G. J. *J. Appl. Crystallogr.* **1988**, *21*, 471–483.
(23) Lehmann, M. S.; Larsen, F. K. *Acta Crystallogr.* **1974**, *A30*, 580–584.
(24) Brown, J. P.; Matthewman, J. C. *The Crystallographic Subroutine Library*; RL-81-063, 1981.
(25) André, D.; Fourme, R.; Renaud, M. *Acta Crystallogr.* **1972**, *A28*, 458–463.
(26) Busing, W. R.; Martin, K. O.; Levy, H. A. *ORFLS4 ORNL*; 59-4-37, Oak Ridge National Laboratory, Oak Ridge, TN, 1971.

Table II. Experimental Parameters of the Neutron Data Collection

	1	2	
orientation	$\vec{a}$	$\vec{a}+\vec{c}$	$\vec{c}-\vec{b}$
cryst dimen (mm)	1.6 × 2.1 × 1.5	1.7 × 1.3 × 0.5	1.2 × 1.0 × 0.6
temp (K)	10	13	13
monochromator		copper	
wavelength (Å)	1.176	1.175	1.175
scan mode		$w/x-\Theta$	
		x[0, 2]	
no. of points	31	29	29
scan width	11	2.2, 3.6	
compt time (cps)		20000	
no. of reflcns	888	973	658
sin Θ/λ_{max}	0.74	0.65	0.43
h	$-4 < h < 1$	$-15 < h < 9$	$-9 < h < 8$
k	$-10 < k < 10$	$0 < k < 13$	$-8 < k < 7$
l	$-10 < l < 10$	$-10 < l < 14$	$-7 < l < 9$
test reflcns	0,3,1	2,0,−2	0,2,2
no. of independent reflcns	616	931	588
agreement R		0.089	
R_w	0.124	0.072	
χ^2	1.05	2.46	

Table III. Selected Bond Lengths (Å) and Angles (deg) for **1** and **2**

	Compound **1**		
Cu1–O1	1.987(40)	Cu1–O2	2.012(39)
Cu1–O5	2.391(36)	Cu2–O3	1.993(37)
Cu2–O4	1.859(47)	Cu2–O6	2.558(32)
O5–N1	1.299(18)	O6–N2	1.273(18)
O1–Cu1–O2	87.0(1.7)	O1–Cu1–O2	93.0(1.7)
O1–Cu1–O5	85.8(1.5)	O1–Cu1–O5	94.2(1.5)
O2–Cu1–O5	84.8(1.4)	O3–Cu2–O4	85.3(2.0)
O3–Cu2–O6	96.3(1.3)	O4–Cu2–O6	102.4(1.4)
Cu1–O5–N1	134.0(2.1)	Cu2–O6–N2	111.5(2.2)
	Compound **2**		
Cu–C1	2.189(18)	Cu–O1	1.985(54)
O1–N1	1.297(19)	O2–N2	1.268(23)
C1–Cu–O1	86.5(0.3)	Cu–O1–N1	123.4(1.6)

package of programs.[27] Corrections included imperfect polarization of the neutron beam.

$(Cu(hfac)_2NITMe)_n$, 1. A crystal was oriented with $\vec{a}$ vertical. Data were collected at 2.5 K following a preliminary study of the 020 reflection which showed a reduction of the magnetic signal below this temperature probably due to interchain interactions.[28] The data were corrected for the nuclear polarization of the hydrogen nuclei.

$CuCl_2(NITPh)_2$, 2. The experiment was performed at 13 K (maximum of the magnetic susceptibility) using a large crystal (see Table IV) in different orientations. In this case, data reduction did not take into account the hydrogen nuclear polarization which is negligible at this temperature.

Experimental conditions concerning polarized neutron data collection are summarized in Table IV; flipping ratios and magnetic structure factors are found in Tables S10 and S11 deposited as supplementary material.

Results

Low-Temperature Structures. $(Cu(hfac)_2NITMe)_n$, 1. The low temperature structure of this complex is shown in Figure 2. Although the overall room temperature structural features such as the chain arrangement including two different copper centers are retained, the tremendous shortening of the c parameter upon cooling induces significant modification of intra- as well as intermolecular arrangements. These modifications are illustrated in Table V where torsion angles within the different cycles and angles between selected planes are reported at high and low temperatures. It is interesting to note that whereas the hexafluoroacetylacetonato rings are almost planar at room temperature,[16] they are considerably distorted at 10 K. This is easily understood if one keeps in mind that the chains are aligned along the $\vec{b}$ direction and that the main axis of the substituted acetylacetonato fragments is directed along $\vec{c}$. Therefore, concomitantly to the shortening of this parameter, these bulky six-membered rings must fold in order to accommodate the diminution of space between the chains. At the same time, the nitroxide fragment which is roughly located in the ab plane is only indirectly influenced by the variation in the c parameter value and has an almost unchanged conformation. Differences between room and low temperature structures are also reflected in some bond lengths. The Cu–O(hfac) bonds are slightly longer than those observed at room temperature probably as a consequence of the folding of the acetylacetonato fragments which results in weaker delocalization. Similar lengthening of Cu–O bonds is observed for the nitroxide binding; in this case, it is likely that the slight increase of the b parameter value (see Table I) upon cooling is related to a larger bonding distance since the Cu–O(nitroxide) bonds are almost collinear with this direction. However, the overall low-temperature-bonding pattern of the Cu ions is almost the same as that found at room temperature as shown by similar bond angles in the two structural determinations.

Table IV. Experimental Parameters of the Polarized Neutron Data Collection

	1	2	
orientation	$\vec{a}$	$\vec{a}+\vec{c}$	$\vec{c}-\vec{b}$
cryst dim (mm)	4.8 × 2.5 × 2.5	6.6 × 5 × 1.3	
temp (K)	2.5	13	
magnetic field (T)		4.6	
monochromator		Fe–Co/Er	
wavelength	0.843	0.980	
polarization		0.980	
flipping efficiency		1	
$\lambda/2$ ratio		0	
no. of data	655	308	264
sin Θ/λ_{max}	0.47	0.65	0.43
h	$-4 < h < 0$	$-15 < h < 13$	$-5 < h < 9$
k	$-12 < k < 11$	$-11 < k < 13$	$-7 < k < 7$
l	$-7 < l < 7$	$-13 < l < 14$	$-8 < l < 5$
no. of independent reflcns	162	145	82

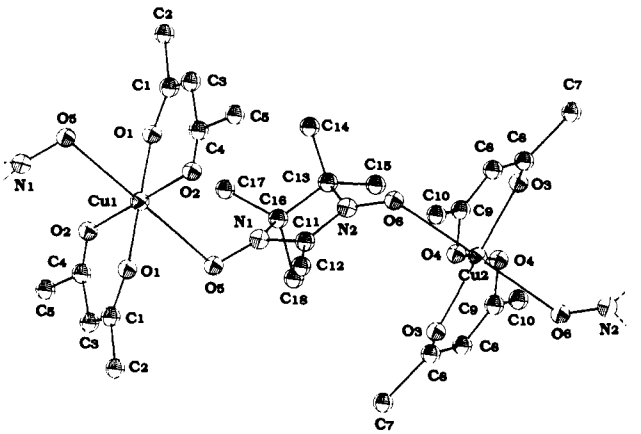

Figure 2. View of the structure of $(Cu(hfac)_2NITMe)_n$ (**1**) showing the numbering of the atoms. Fluorine and hydrogen atoms have been omitted. Thermal ellipsoids are drawn at the 90% probability level.

$CuCl_2(NITPh)_2$, 2. Inspection of bond lengths and angles (Table III) shows that the low-temperature structure of $CuCl_2(NITPh)_2$ is identical, within experimental error, to that already reported at room temperature (Figure 3).[12] However, neutron diffraction, which allows precise determination of the hydrogen atom positions, gives useful information about the conformation of the nitroxide fragment. As expected, the hydrogen atoms of the methyl groups are staggered. All other structural features are as previously described and need no further comment.

(27) Delapalme, A. Thesis, Université de Grenoble, 1967. Tasset, F. Thesis, Université de Grenoble, 1975.

(28) Cabello, C. I.; Caneschi, A.; Carlin, R. L.; Gatteschi, D.; Rey, P.; Sessoli, R. *Inorg. Chem.* **1990**, *29*, 2582–2587.

Table V. Torsion Angles within Cycles and Angles between Selected Planes at High and Low Temperature in **1**

	T = 10 K	room temp
Cu1–O1–C1–C3	−29.2	−9.4
O1–C1–C3–C4	17.9	0.5
C1–C3–C4–O2	11.8	3.2
C3–C4–O2–Cu1	−19.3	3.0
C4–O2–Cu1–O1	6.1	−8.4
O2–Cu1–O1–C1	14.4	11.2
Cu2–O3–C6–C8	−28.5	−12.8
O3–C6–C8–C9	8.1	−2.5
C6–C8–C9–O4	1.4	3.4
C8–C9–O4–Cu2	11.8	11.1
C9–O4–Cu2–O3	−20.7	−18.8
O4–Cu2–O3–C6	30.4	19.6
N1–C11–N2–C13	15.1	11.4
C11–N2–C13–C16	−28.3	−22.5
N2–C13–C16–N1	26.2	22.8
C13–C16–N1–C11	−19.8	−19.3
C16–N1–C11–N2	3.4	5.7

	plane 1	plane 2	plane 3	plane 4
plane 2	44.8 (51.5)			
plane 3	55.3 (55.8)	45.9 (51.9)		
plane 4	60.0 (62.9)	48.0 (52.6)	4.7 (7.7)	
plane 5	57.5 (57.5)	59.3 (61.5)	14.8 (10.1)	16.0 (14.2)

plane 1: Cu1–O1–O2–C1–C3–C4
plane 2: Cu2–O3–O4–C6–C8–C9
plane 3: O5–N1–C11–N2–O6
plane 4: N1–C11–C16
plane 5: N2–C11–C13

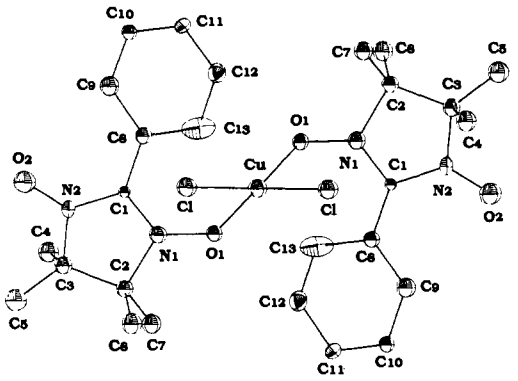

Figure 3. View of the structure of $CuCl_2(NITPh)_2$ (**2**) showing the numbering of the atoms. Hydrogen atoms have been omitted. Thermal ellipsoids are drawn at the 90% probability level.

Spin Densities. For centrosymmetric cells, spin densities are usually obtained by direct methods, namely Fourier transformation and maximum entropy analysis.[29] In contrast, indirect methods such as multipole[30] or wave function modeling[31] can be used independent of the symmetry. According to our experience with nitroxides[18,32,33] and related free radicals,[34] it seems that a wave function analysis would be the most appropriate method; this was verified by performing the four data treatments on compound **2**.

Since in these complexes the metal ground state is nondegenerate, it was reasonable to assume that there was no orbital contribution to the magnetization. In this spin-only scheme, the spin density is proportional to the mean-squared value of the total magnetic molecular orbital and the magnetic structure factors are obtained by Fourier transform of this function.[21]

Let us expand the unpaired electron molecular orbital onto an atomic orbital basis set:

$$\psi = \sum_i (\mu_i)^{1/2} \sum_j a_{ij}\varphi_{ij}$$

where i runs over the atoms and j over the atomic orbitals φ_{ij} centered on atom i. The μ_i's are the spin populations carried by the different atoms and the a_{ij}'s are the φ_{ij} coefficients; the a_{ij}'s are normalized through the condition

$$\sum_j a_{ij}^2 = 1$$

The magnetic structure factors are defined as

$$F_M(\vec{K}) = \langle\psi|e^{i\vec{K}\vec{r}}|\psi\rangle$$

Neglecting the two-center integrals, $F_M(\vec{K})$ may be written as

$$F_M(\vec{K}) = \sum_i \mu_i f_i(\vec{K}) e^{i\vec{K}\vec{r}_i} e^{-W_i}$$

where $f_i(K)$ and r_i represent the so-called form factor and the position in the cell of atom i, respectively; e^{-W_i} takes into account the thermal motion. If the φ_{ij}'s are defined as classical Slater type orbitals

$$\varphi_{ij}(\vec{r}) = \sum_l R_i^l(r) \sum_{m=-l}^{+l} c_l^m Y_l^m(\vec{r})$$

one ends up with the following expression of the form factor

$$f_i(\vec{K}) = \sum_L \langle j_L(\vec{K})\rangle \sum_M C_L^M Y_L^{M'}(\hat{K})$$

where

$$C_L^M = i^L(2L'+1)[4\pi(2L+1)]^{1/2} \times \begin{pmatrix} L' & L' & L \\ 0 & 0 & 0 \end{pmatrix} \sum_{M',M''} (-1)^M \begin{pmatrix} L' & L' & L \\ -M' & M'' & M \end{pmatrix} c_{L'}^{M'*} c_{L''}^{M''}$$

and where

$$\begin{pmatrix} L' & L' & L \\ 0 & 0 & 0 \end{pmatrix} \text{ and } \begin{pmatrix} L' & L' & L \\ -M' & M'' & M \end{pmatrix}$$

are the coefficients involved in the calculations of the product of three spherical harmonics. The $j_L(\vec{K})$ functions are defined as

$$\langle j_L(\vec{K})\rangle = \int_0^\infty R_1^L(r)^2 j_L(Kr) r^2\, dr$$

The parameters of the model (μ_i, a_{ij}, and the radial exponents) are fitted to the experimental data using a least-squares procedure.

$(Cu(hfac)_2NITMe)_n$, 1. Figure 4 shows the projection of the spin density along the π direction of the radical as obtained from a wave function analysis. Seven atoms (the five-membered ring and the two oxygen atoms) of the free radical and the copper ion surrounded by the coordinated oxygen atoms were included in the calculations. Both the spin populations and the coefficients of the atomic orbitals were refined making the following approximations: (i) The unpaired electron on both copper sites is correctly described by linear combinations of 3d orbitals. (ii) For the two NO groups of the radical fragment, only the 2s, $2p_x$, $2p_y$, and $2p_z$ atomic orbitals are taken into account. (iii) For the carbon atoms and the hexafluoroacetylacetonate oxygens only the spherical contributions to the molecular wave function are refined. Table VI lists the unpaired spin populations carried by the different atoms, while the coefficients of the atomic orbitals in the molecular orbital are found in Table VII. Important to

(29) Papoular, R.; Schweizer, J. *Proceedings of the VI International School of Neutron Physics, Alushta*, **1990**, 170–189.
(30) Papoular, R.; Gillon, B. *Neutron Scattering Data Analysis*; **1990**, *107*, 101–116.
(31) Ressouche, E. Thesis, Université de Grenoble, 1991.
(32) Brown, P. J.; Capiomont, A.; Gillon, B.; Schweizer, *J. Mol. Phys.* **1983**, *48*, 753–761.
(33) Gillon, B. Thesis, Université de Grenoble, 1983.
(34) Boucherle, J.-X.; Gillon, B.; Maruani, J.; Schweizer, J. *Mol. Phys.* **1987**, *60*, 1121–1142.

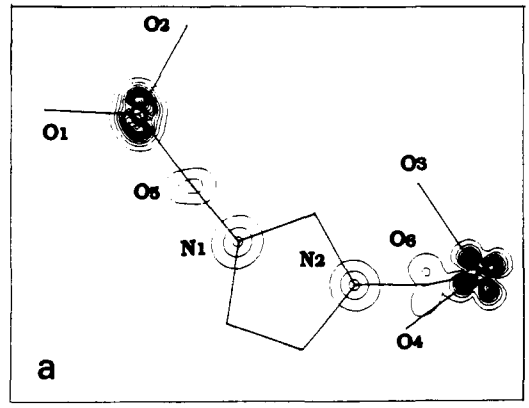

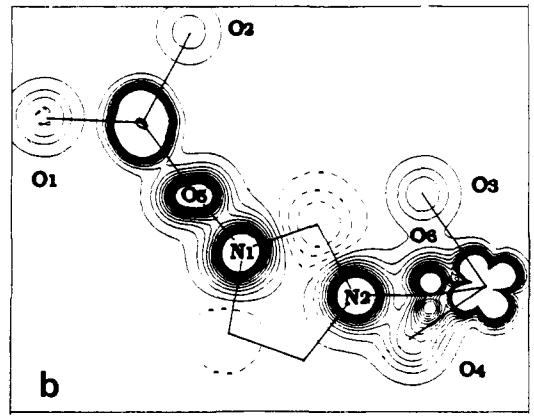

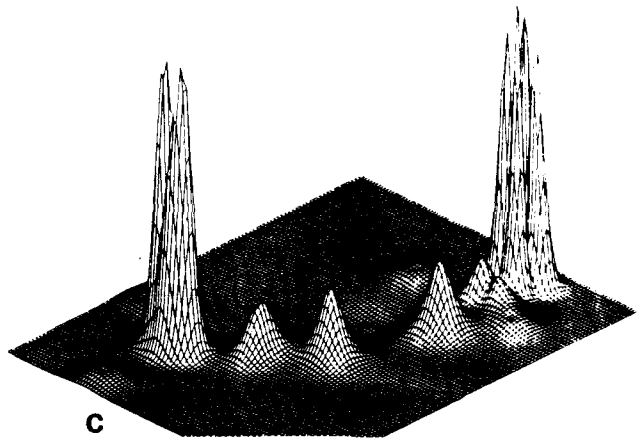

Figure 4. Projection of the spin density along the π^* direction of the nitroxide in $(Cu(hfac)_2NITMe)_n$, (**1**): (a) high-contour map, $100 \pm n(200)$ $m\mu_B/Å^2$; (b) low-contour map, $5 \pm n(10)$ $m\mu_B/Å^2$; (c) spatial representation.

Table VI. Atomic Spin Populations (μ_B) in **1**

Cu1	0.858(9)	O6	0.190(10)	O2	0.059(6)
Cu2	0.754(8)	C11	-0.100(9)	O3	0.051(6)
N1	0.311(8)	C13	0.011(8)	O4	0.073(6)
O5	0.205(7)	C16	-0.040(8)	M^a	1.895(26)
N2	0.299(8)	O1	0.030(6)	χ^2	2.55

[a] Total magnetization.

note is the following: (i) The total value of the spin population (1.895(26) μ_B) is in good agreement with that obtained from magnetization data under the same experimental conditions (1.906 μ_B). (ii) The spin density is positive on the entire molecular backbone except for a weak negative contribution from the carbon atom bridging the NO groups in the radical. (iii) Each fragment (Cu1, Cu2, and the free radical) carries one electron within experimental errors. Table VII gives precise information about spin distribution around the metal ions (Figure 5). Although the spin density is mainly located in the basal plane of the ions ($d_{x^2-y^2}$ and d_{xy}), there is substantial contribution of the d_{yz} orbital to the magnetic environment of Cu2. The magnetic orbital at the free radical is not rigorously parallel to the basal metal plane nor to the normal to the radical mean plane; the different angular parameters describing this arrangement are reported in Figure 5.

$CuCl_2(NITPh)_2$, 2. As the magnetic signal for this compound is weak, additional assumptions were included in the calculation of the wave function. The nature of the contribution of the copper(II) ion was assumed to be $3d_{x^2-y^2}$. As before, only the spherical contribution of the carbon atoms to the molecular orbital has been refined; the same simplification was applied to the chloro ligands. The 2s contribution of the NO groups was neglected and the Slater exponents were not refined. In the maps shown in Figure 6, it is worth noting that the spin density of the copper ion is negative in contrast to the positive spin density on the two nitroxide fragments. The other predominant feature of these maps is that zero density is found on the chloro ligands and more surprisingly zero spin density is even found on the bound nitroxide oxygen atom. Quantitatively, the total spin population (0.056(1) μ_B, see Table VIII) compares fairly well to that deduced from magnetization data (0.061 μ_B) and, more interestingly, the distribution of this population among the different fragments is $^2/_3, -^1/_3, ^2/_3$. Although the overall radical density is positive, a negative contribution of the bridging carbon atom (C11) is found as has already been observed in compound **1**. The coefficients listed in Table IX show the major π character of the nitroxide contribution.

Discussion

For the last 10 years, the polarized neutron diffraction technique has given unique information about spin distribution and bonding properties in coordination compounds.[35,36] Recent studies[37,38] have given a definite insight into magnetic exchange mechanisms in binuclear complexes.

Alternatively, theoretical calculations may give valuable information about molecular compounds. Thus, most of the reported theoretical studies[39,40] give rather good descriptions of the unpaired spin orbital in nitroxides which support most of their observed properties. However, a polarized neutron study of piperidinyl nitroxides[18] has shown that even sophisticated Hartree–Fock theoretical models could not account for precise spin distribution in the molecule; the difficulty of taking into account the perturbations of the NO group through intermolecular interactions was particularly stressed. Concerning metal complexes of these free radicals, sophisticated calculations exceed by far the possibilities of the most powerful computers and only very qualitative pictures are available for understanding the nature of the metal–radical interaction. As mentioned previously, in copper derivatives, the magnitude of these interactions is spread over a large range of energy (-500, +500 cm^{-1}) and one feels intuitively that the differences observed in the spin density maps for **1** and **2** are correlated with the opposite nature of the metal–radical coupling in these two compounds.

Ferromagnetically Coupled Copper–Nitroxide Complexes. Axial ligation of a nitroxide to an octahedral copper ion through the oxygen atom, as observed in $(Cu(hfac)_2NITMe)_n$ (**1**), leads to weak metal–radical ferromagnetic coupling. Numerous derivatives of this class of complexes have been characterized,[9,13-16]

(35) Figgis, B. N.; Reynolds, P. A.; White, A. H. *Inorg. Chem.* **1985**, *24*, 3762–3770.
(36) Figgis, B. N.; Reynolds, P. A.; Forsyth, J. B. *J. Chem. Soc., Dalton Trans.* **1988**, 117–122.
(37) Figgis, B. N.; Mason, R.; Smith, A. R. P.; Varghese, J. N.; Williams, G. A. *J. Chem. Soc., Dalton Trans.* **1983**, 703–711.
(38) Gillon, B.; Cavata, C.; Schweiss, P.; Journaux, Y.; Kahn, O.; Schneider, D. *J. Am. Chem. Soc.* **1989**, *111*, 7124–7132.
(39) Davis, M. S.; Morokuma, K.; Kreilick, R. W. *J. Am. Chem. Soc.* **1972**, *94*, 5588–5592.
(40) Gillon, B.; Becker, P.; Ellinger, Y. *Mol. Phys.* **1983**, *48*, 763–764.

Table VII. Atomic Orbital Coefficients Resulting from Wave Function Analysis of the Spin Density in **1**

	$3d_{z^2}$	$3d_{xz}$	$3d_{yz}$	$3d_{x^2-y^2}$	$3d_{xy}$
Cu1	–0.334(135)	0.049(112)	0.587(171)	–0.604(170)	0.420(83)
Cu2	0.035(160)	0.236(198)	–0.005(148)	0.911(109)	0.338(186)
	Ms[a]	2s	$2p_x$	$2p_y$	$2p_z$
N1	0.010(3)	0.178(27)	–0.401(72)	–0.125(89)	0.890(32)
O5	0.004(3)	–0.146(47)	–0.555(134)	0.287(146)	0.767(88)
N2	0.001(1)	–0.041(26)	–0.115(125)	–0.181(83)	0.976(21)
O6	0.015(7)	–0.278(62)	0.771(65)	–0.017(117)	0.573(70)

[a] Total spin population in the 2s orbital (μ_B).

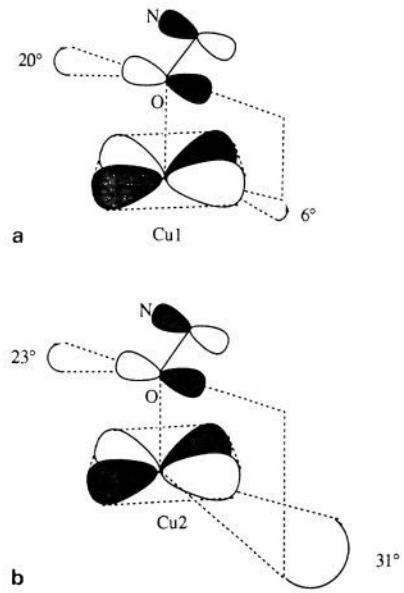

Figure 5. Schematic representation of the magnetic orbitals around the two coordination sites in $(Cu(hfac)_2NITMe)_n$ (**1**) showing the relative orientation of the nitroxide and metal magnetic orbitals: (a) Cu(1) and (b) Cu(2).

and their magnetic properties have been qualitatively rationalized in the frame of extended Huckel calculations.[9]

The crystal structures of this adduct at low temperature as well as at room temperature show the chain arrangement of the alternating metal ions and nitroxide radicals. Although the bond lengths of the bridging radical to the two distinct copper centers are not identical, the magnetic data were fairly well reproduced by using a model involving only one exchange interaction. At low temperature, the decrease of the magnetic signal of the 020 reflection below 2.5 K agrees with magnetic measurements and confirms that the compound does not order ferromagnetically.[28]

As expected for ferromagnetic interactions, the spin density distribution in this compound (Figure 4) shows only positive values except for a weak but significant negative contribution due to spin polarization on the bridging sp^2 carbon of the radical. The two NO groups carry equal spin density which is unequally distributed over the nitrogen and oxygen. While both atoms are expected to bear equal density in the uncoordinated ligand,[41] in the complex, the nitrogen carries 50% more spin density than the oxygen (see Table VII). This result nicely supports previous structural and spectroscopic observations. Solution EPR studies of nitroxides have shown a strong dependence of the nitrogen hyperfine splitting on the nature of the solvent. Indeed, solvation of the oxygen atom by polar solvents favors the polar limit formula in which more spin density on the nitrogen leads to an increase of the splitting. A similar feature was the main result of a polarized neutron diffraction study of Tempol where, in the solid state, the

(41) Preliminary results of a polarized neutron diffraction study do show that in NITPh (see Figure 1) the atoms of the NO groups carry equal spin populations.

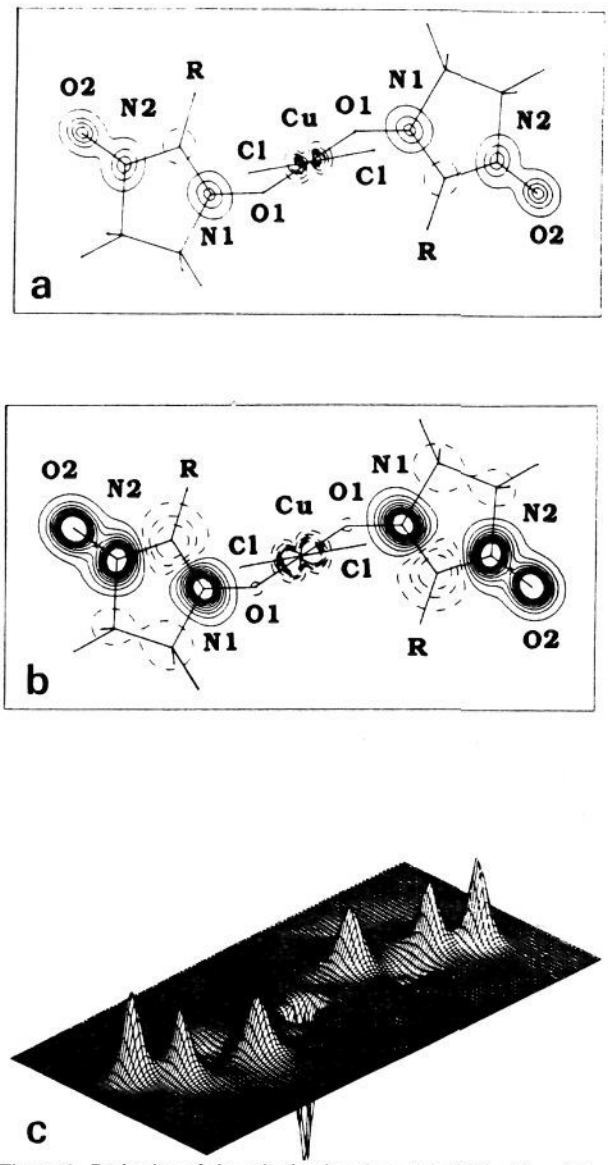

Figure 6. Projection of the spin density along the π^* direction of the nitroxide in $CuCl_2(NITPh)_2$, **2**: (a) high-contour map, $100 \pm n(200)$ $m\mu_B/Å^2$; (b) low-contour map, $5 \pm n(10)$ $m\mu_B/Å^2$; (c) spatial representation.

NO group is involved in hydrogen bonding.[18] More important qualitative information about the modification of spin distribution in metal-bound nitroxides comes from EPR studies of complexes with diamagnetic group III halides.[19] In addition to an increase of the nitrogen splitting, a modification of the spin distribution involving the metal center is observed, giving rise to extra hyperfine coupling when the metal ion has a nuclear spin. Although diamagnetic, these metal centers are strong Lewis acids which, in this respect, resemble the metal–hexafluoroacetylacetonates

Table VIII. Atomic Spin Populations (μ_B) in **2**

Cu	−0.020(2)	N2	0.018(2)	C2	−0.003(2)
Cl	−0.001(3)	O2	0.019(2)	C3	−0.002(2)
N1	0.017(2)	C1	−0.010(2)	M[a]	0.056(12)
O1	0.000(2)			χ^2	1.05

[a] Total magnetization.

Table IX. Atomic Orbital Coefficients Resulting from Wave Function Analysis of the Spin Density in **2**

	$3d_{z^2}$	$3d_{xz}$	$3d_{yz}$	$3d_{x^2-y^2}$	$3d_{xy}$
Cu[a]	0	0	0	1	0
	$2p_x$		$2p_y$	$2p_z$	
N1	0.313(225)		0.285(326)	0.906(115)	
O1[a]	0		0	1	
N2	0.534(178)		0.250(229)	0.808(116)	
O2	0.202(306)		0.470(249)	0.859(140)	

[a] Not refined.

used in the present study. Therefore, this transfer of spin density is related to the familiar limit formula in which the unpaired spin is localized on the nitrogen. In this model, the nitrogen and oxygen atoms are singly bonded so that a lengthening of the NO bond might be expected. Since in **1** the nitroxide is weakly bound (Cu–O(nitroxyl) > 2.3 Å) no lengthening is observed; in strongly interacting species such as compound **2**, however, the coordinated NO group does show a lengthening of ca. 0.03 Å.

In addition to this transfer of spin density from oxygen to nitrogen, it is important to note that the nitroxide magnetic orbital deviates notably from the ideal π^* direction perpendicular to the mean plane of the ligand. Furthermore, the oxygen and nitrogen contributions are not parallel as would be expected in the uncoordinated species. For the first metal site (Cu2), where the magnetic orbital has predominant $d_{x^2-y^2}$ and d_{xy} character, the nitroxide spin population is roughly parallel to the metal basal plane resulting in a very weak overlap. Such a situation which favors a ferromagnetic interaction is also found in the second site (Cu1): although a more complicated orbital scheme including a significant d_{yz} contribution is observed, the overlap of the magnetic orbitals is again minimized because the nitroxide orbital is precisely directed along the x axis. Therefore, the ferromagnetic behavior of this compound is consistent with the scheme of accidental orthogonality of magnetic orbitals.[42]

However, another coupling mechanism involving delocalization of ligand unpaired spin into the metal d_{z^2} orbital has recently been proposed.[43] Indeed, the bonding geometry of the ligand does not generally match the idealized axial coordination pattern (Cu–O–N = 180°), so that overlap between the π^* nitroxide orbital and the d_{z^2} copper orbital might be considered as an efficient coupling pathway. In addition, π back-bonding involving the d_{xz} and d_{yz} orbitals which is symmetry allowed in this coordination geometry may play the same role. A similar delocalization model has been suggested to explain the ferromagnetic behavior of rare earth–nitroxide complexes.[44] Although ab initio calculations support this model,[43] current studies in this field have demonstrated the difficulty of obtaining reliable coupling constants in large molecules.[45] Our study does not bring a definite answer to this question since the data are not accurate enough to allow a description of ligand-to-metal spin delocalization. However, the spin densities carried by each fragment strongly suggest that the mechanism involving orthogonal magnetic orbitals is predominant.

Antiferromagnetically Coupled Complexes. Most of the copper(II) adducts of this class, such as $Cu(hfac)_2$Tempo which is the first fully characterized copper–nitroxide complex,[4] are so strongly coupled that they often exhibit a singlet ground state even at room temperature. However, $CuCl_2(NITPh)_2$ being a three-spin system, the spin state of lowest multiplicity is a doublet and a spin density determination was possible.

Simple quantum mechanical considerations give a description of the different states of the molecule. Let us consider the spin Hamiltonian of such a centrosymmetric three-spin system

$$H = -2J(\vec{s}_1\vec{s}_M + \vec{s}_M\vec{s}_2) - 2J'\vec{s}_2\vec{s}_1$$

where s_1 and s_2 stand for the spin operators of the radicals and s_M for that of the metal ion and J and J' are the copper–nitroxide and the nitroxide–nitroxide interactions, respectively. The Heitler–London type eigenfunctions corresponding to the eigen states of S^2 may be written as

$$\Phi_{\text{doublet(1)}} = {}^1/_6(2|\phi_1\bar{\phi}_M\phi_2| - |\bar{\phi}_1\phi_M\phi_2| - |\phi_1\phi_M\bar{\phi}_2|)$$

$$\Phi_{\text{doublet(2)}} = \left(\frac{1}{2\sqrt{3}}\right)(|\phi_1\phi_M\bar{\phi}_2| - |\bar{\phi}_1\phi_M\phi_2|)$$

$$\Phi_{\text{quartet}} = \left(\frac{1}{3\sqrt{2}}\right)(|\phi_1\phi_M\bar{\phi}_2| + |\bar{\phi}_1\phi_M\phi_2| + |\phi_1\phi_M\bar{\phi}_2|)$$

where the ϕ_i's are the magnetic orbitals of the different fragments, $|\phi_1\phi_M\phi_2|$ is a Slater determinant, and the bar stands for a β spin. The spin density of each state is calculated as

$$\rho(r_o) = 1/M_S\sum_i S_i^z\delta(r_i - r_o)$$

Considering only the doublet states, the distribution of the spin density is ${}^2/_3$ on the nitroxide and $-{}^1/_3$ on the metal ion for doublet(1), while it is 0 on the nitroxide and 1 on the copper ion for doublet(2).

Confirmation of a doublet ground state came from EPR spectra and magnetic susceptibility measurements in the range of 50–300 K which also showed that the excited quartet state is not populated even at room temperature. The g values of the two possible doublet states are $g = (4g_{NO} - g_{Cu})/3$ for doublet(1) and $g = g_{Cu}$ for doublet(2).[46] In giving a g value lower than 2, both magnetic and EPR data consistently suggest that the actual ground state of the molecule is doublet(1).

At lower temperatures, deviation from Curie behavior is observed since intermolecular antiferromagnetic interactions become operative.[12] Accordingly, at the temperature and field of the polarized neutron diffraction experiment (13 K, 4.6 T), a magnetization value of 0.06 μ_B is observed, which is much weaker than that predicted by the Brillouin function associated with a spin ${}^1/_2$ (0.23 μ_B). Full-scale magnetization could be obtained on applying a much stronger field; the coupling between the molecules acts as a normalizing factor reducing the total amount of polarized spin.

Notwithstanding the reduced magnetic signal, experimental spin populations on the different fragments (Table VIII) are exactly those expected for doublet(1): $+{}^2/_3$ for the organic radicals and $-{}^1/_3$ for the copper ion. It is worth noting that the ratio of these populations is exactly the same as that involved in the determination of the g factor of doublet(1). This remarkable agreement shows that even with a low magnetic signal, the polarized neutron diffraction technique is able to give valuable quantitative data.

In addition to the assessment of the ground state, the distribution of the spin density in each fragment (except for the description of the Cu(II) ion which was assumed to be $d_{x^2-y^2}$ at the very beginning) gives important information about bonding in these compounds. For instance, the absence of spin density on the

(42) Kahn, O.; Charlot, M. F. *Nouv. J. Chim.* **1980**, *4*, 567–576.
(43) Musin, R. N.; Shastnev, P. V.; Malinovskaya, S. A. *Inorg. Chem.* **1992**, *31*, 4118–4121.
(44) Benelli, C.; Caneschi, A.; Gatteschi, D.; Rey, P. *Inorg. Chem.* **1989**, *28*, 3230–3234.
(45) De Loth, P.; Cassoux, P.; Daudey, J. P.; Malrieu, J. P. *J. Am. Chem. Soc.* **1981**, *103*, 4007–4016.
(46) Gatteschi, D.; Bencini, A. *Magneto-Structural Correlations in Exchange Coupled Systems*; Willet, R. D., Gatteschi, D.; Kahn, O., Eds.; Noato Asi Series, 140, D. Reidel Publishing Co.: Dordrecht, The Netherlands, 1985; pp 241–268.

halogen centers is probably the signature of the predominant ionic character of the copper–chlorine bond. Concerning the nitroxide moieties, the zero spin density on the coordinated oxygen atom is a most salient feature. Surprising this result is in line with spin density transfer within the NO group as observed in compound **1**, and it agrees with the observed large lengthening of the NO bond of ca. 0.03 Å induced by strong binding to the metal ion (Cu–O = 1.985(54) Å). Further agreement comes from the uniform spin distribution and the regular bond length observed in the uncoordinated NO group. However, if weaker spin density is expected on the bound oxygen, a zero value may be accidental and due to compensation of contributions of opposite sign as observed on the bridging atom in a heteronuclear complex.[38]

Finally, the projection of the molecular wave function on the atomic orbitals (Table IX) shows that spin density in the nitroxide ligands has predominant $2p_z$ character in agreement with the familiar π^* picture. Due to the binding geometry characterized by a Cu–O–N angle close to 120° and a Cu–O–N plane perpendicular to the nitroxide mean plane, this representation strongly supports the naive geometric representation of the overlap of the magnetic orbitals which allows for the qualitative interpretation of the antiferromagnetic properties in these systems.

Concluding Remarks

Compelling evidence for strong modification of the starting electronic structure of the fragments upon coordination is the main result of this work. Determination of the spin density allows assessment of the ground state and a precise description of the metal–radical coupling in these complexes. It is clearly observed that coordination of a nitroxide to a copper(II) ion results in spin density transfer from the bound oxygen atom to the nitrogen. Although π-back-bonding and delocalization do not seem to play a major role in metal–nitroxide binding, a better understanding of the bonding properties will be reached when the charge density in **2** is determined (work in progress).

Attempts to rationalize our results using available calculation frames were unsuccessful. The main difficulty of such studies is the size of the molecules. Concerning $(Cu(hfac)_2NITMe)_n$, realistic calculations must include the chain character of the compound in periodical limit conditions, a possibility which is not included in the available softwares. On the other hand, taking into account the symmetry, it was found that $CuCl_2(NITPh)_2$ could be investigated neglecting the substituting groups of the ligands. Preliminary calculations showed some qualitative agreement in giving unequal spin distribution within the bound NO group. However, the approximations were probably too severe since the experimental spin distribution could not be quantitatively reproduced.

Acknowledgment. Reviewing of the manuscript by Dr. D. E. OVER is gratefully acknowledged.

Supplementary Material Available: Atomic positional parameters (Tables S1, S2), bond lengths (Table S3), and angles (Table S4) for **1**, bond lengths (Table S5) and bond angles (Table S6) for **2**, anisotropic thermal parameters (Table S7) for **2** (8 pages); observed and calculated structure factors (Tables S8-9) and magnetic structure factors (Tables S10-11) for **1** and **2**, respectively (20 pages). Ordering information is given on any current masthead page.